Phosphorylation of synaptotagmin-1 controls a post-priming step in PKC-dependent presynaptic plasticity

Arthur P. H. de Jong[a,1], Marieke Meijer[a,b], Ingrid Saarloos[b], Lennart Niels Cornelisse[b], Ruud F. G. Toonen[a], Jakob B. Sørensen[c,d], and Matthijs Verhage[a,b,2]

[a]Department of Functional Genomics, Center for Neurogenomics and Cognitive Research, Neuroscience Campus Amsterdam, VU University and VU Medical Center, Amsterdam 1081HV, The Netherlands; [b]Department of Clinical Genetics, Center for Neurogenomics and Cognitive Research, Neuroscience Campus Amsterdam, VU University and VU Medical Center, Amsterdam 1081HV, The Netherlands; [c]Department of Neuroscience and Pharmacology, Faculty of Health Sciences, University of Copenhagen, Copenhagen DK-2200, Denmark; and [d]Lundbeck Foundation Center for Biomembranes in Nanomedicine, University of Copenhagen, Copenhagen DK-2200, Denmark

Edited by Reinhard Jahn, Max Planck Institute for Biophysical Chemistry, Goettingen, Germany, and approved March 22, 2016 (received for review November 19, 2015)

Presynaptic activation of the diacylglycerol (DAG)/protein kinase C (PKC) pathway is a central event in short-term synaptic plasticity. Two substrates, Munc13-1 and Munc18-1, are essential for DAG-induced potentiation of vesicle priming, but the role of most presynaptic PKC substrates is not understood. Here, we show that a mutation in synaptotagmin-1 (Syt1^{T112A}), which prevents its PKC-dependent phosphorylation, abolishes DAG-induced potentiation of synaptic transmission in hippocampal neurons. This mutant also reduces potentiation of spontaneous release, but only if alternative Ca^{2+} sensors, Doc2A/B proteins, are absent. However, unlike mutations in Munc13-1 or Munc18-1 that prevent DAG-induced potentiation, the synaptotagmin-1 mutation does not affect paired-pulse facilitation. Furthermore, experiments to probe vesicle priming (recovery after train stimulation and dual application of hypertonic solutions) also reveal no abnormalities. Expression of synaptotagmin-2, which lacks a seven amino acid sequence that contains the phosphorylation site in synaptotagmin-1, or a synaptotagmin-1 variant with these seven residues removed (Syt1$^{\Delta 109-116}$), supports normal DAG-induced potentiation. These data suggest that this seven residue sequence in synaptotagmin-1 situated in the linker between the transmembrane and C2A domains is inhibitory in the unphosphorylated state and becomes permissive of potentiation upon phosphorylation. We conclude that synaptotagmin-1 phosphorylation is an essential step in PKC-dependent potentiation of synaptic transmission, acting downstream of the two other essential DAG/PKC substrates, Munc13-1 and Munc18-1.

synaptotagmin | short-term plasticity | protein kinase C | diacylglycerol | Doc2

Presynaptic strength changes rapidly during repetitive stimulation [short-term plasticity (STP)] and activation of intracellular signal transduction pathways (1, 2). The diacylglycerol (DAG)/protein kinase C (PKC) cascade is one of the most potent pathways at the presynaptic terminal. Its activation leads to 50–100% potentiation of spontaneous and action potential (AP)-evoked release (3–5), and is critical for multiple forms of presynaptic plasticity (6–8). DAG directly activates the vesicle priming factor Munc13-1 (9, 10) and indirectly activates downstream effectors via PKC. Activation of both Munc13-1 and PKC is essential for this pathway to operate (Fig. 1*A*) (8, 11). We previously identified Munc18-1 as an essential PKC substrate, because a nonphosphorylatable Munc18-1 mutant completely inhibits PKC-dependent STP (8, 12). Importantly, a phosphomimetic mutation of Munc18-1 cannot fully bypass the requirement for PKC activation, indicating that other PKC substrates must contribute to this form of plasticity (8). These substrates have not been identified to date.

Among other presynaptic PKC substrates is synaptotagmin-1 (Syt1, ref. 13). Syt1 is the vesicular Ca^{2+} sensor that mediates fast AP-evoked release in the hippocampus (14) and drives a large fraction of spontaneous release (15). In the latter case, Syt1 competes with alternative sensors, in particular Doc2s, for SNARE binding and the initiation of vesicle fusion (16, 17). Syt1 bears a highly conserved phosphorylation site (threonine 112) in a putative α-helix in the linker between the transmembrane (TM) and C2A domain that can be phosphorylated by PKC and Ca^{2+}/calmodulin (CaM)-dependent protein kinase II (CaMK-II, refs. 13 and 18). The Syt1 homologs Syt7 and Syt12 contain similar phosphorylation sites in the linker between TM and C2A, and their phosphorylation potentiates Ca^{2+}-induced vesicle fusion (19, 20). Unexpectedly, a nonphosphorylatable Syt1 variant had no effect on vesicle fusion in mouse embryonic chromaffin cells (21). However, we previously observed only limited contribution of PKC in mouse embryonic chromaffin cells compared with adult bovine chromaffin cells and neurons (8, 22), suggesting that the role of PKC may differ between model systems.

In the current study, we investigated the effect of phosphorylation of Syt1 by PKC on synaptic transmission in mouse hippocampal neurons. We found that the nonphosphorylatable Syt1 mutant abolished potentiation of evoked release induced by synthetic DAG analogs and severely reduced the potentiation after high-frequency stimulation. Surprisingly, paired-pulse facilitation and vesicle replenishment were not affected when the Syt1 phosphorylation site was modified. We conclude that phosphorylation of Syt1 acts downstream of vesicle priming to control synaptic plasticity.

Significance

Synapses can be temporarily strengthened by bursts of action potentials, which are thought to be a central aspect of information processing in the brain. This study provides evidence that protein kinase C (PKC)-dependent phosphorylation of synaptotagmin-1 is an essential step in this strengthening. A mutation that prevents synaptotagmin-1 phosphorylation abolishes this strengthening, both after action potential bursts and upon direct PKC activation by a synthetic analog of diacylglycerol, whereas basal synaptic transmission is unaffected. This suggests that synaptotagmin-1 acts in a cooperative fashion with Munc18-1 and Munc13-1, which were previously identified as essential diacylglycerol/PKC substrates. Together these data identify a central pathway linking bursts of action potentials to enhanced synaptic strength.

Author contributions: A.P.H.d.J., R.F.G.T., J.B.S., and M.V. designed research; A.P.H.d.J., M.M., and I.S. performed research; A.P.H.d.J., M.M., I.S., L.N.C., R.F.G.T., J.B.S., and M.V. analyzed data; and A.P.H.d.J. and M.V. wrote the paper.

The authors declare no conflict of interest.

This article is a PNAS Direct Submission.

[1]Present address: Department of Neurobiology, Harvard Medical School, Boston, MA 02115.

[2]To whom correspondence should be addressed. Email: matthijs@cncr.vu.nl.

This article contains supporting information online at www.pnas.org/lookup/suppl/doi:10.1073/pnas.1522927113/-/DCSupplemental.

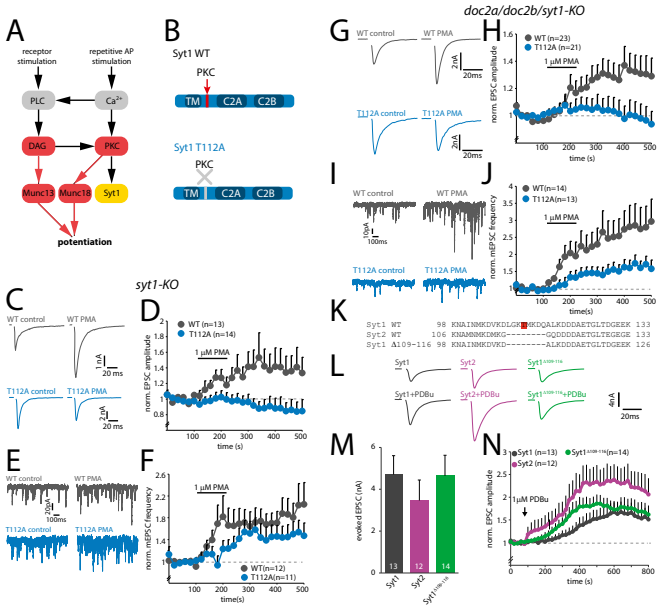

Fig. 1. Phosphorylation of T112 is essential for phorbol-ester–induced potentiation of vesicle release. (*A*) Schematic overview of the DAG/PKC pathway. Phospholipase C (PLC) is activated by receptor stimulation or elevated Ca^{2+} levels, leading to the production of DAG. DAG activates Munc13 and PKC, whereas PKC phosphorylates Munc18 and Syt1. Essential events are indicated in red. The role of Syt1 phosphorylation is the subject of the current study. (*B*) Schematic representations of Syt^{WT} and Syt^{T112A} constructs. TM, transmembrane domain. (*C*) Typical examples of AP-evoked release in control and after superfusion with 1 µM PMA. (*D*) Change in average normalized evoked EPSC amplitude induced by PMA. APs were evoked at 0.05 Hz ($n = 3$). (*E*) Typical examples of miniature EPSCs (mEPSCs) in control and after superfusion with PMA. (*F*) Change in average normalized mEPSC frequency induced by PMA ($n = 3$). (*G*) Typical examples of AP-evoked release in TKO neurons rescued with Syt^{WT} and Syt^{T112A} in control and after superfusion with 1 µM PMA. (*H*) Change in average normalized evoked EPSC amplitude induced by PMA in TKO cells. APs were evoked at 0.05 Hz ($n = 4$). (*I*) Typical examples of mEPSCs in TKO cells rescued with Syt^{WT} or Syt^{T112A} in control and after addition of PMA. (*J*) Changes in average normalized mEPSC frequency induced by PMA in TKO cells ($n = 4$). (*K*) Sequence alignment comparing rat $Syt1^{WT}$, $Syt2^{WT}$, and $Syt1^{\Delta 109–116}$. T112 in $Syt1^{WT}$ is highlighted in red. (*L*) Typical examples of AP-evoked release in Syt1 KO cells rescued with $Syt1^{WT}$, $Syt2^{WT}$, or $Syt1^{\Delta 109–116}$. (*M*) Average AP-evoked EPSC amplitude ($n = 6$). (*N*) Change in average normalized evoked EPSC amplitude induced by 1 µM PDBu ($n = 6$).

Results

Phosphorylation of T112 Is Essential for Phorbol Ester-Induced Potentiation of Release. To test if phosphorylation of Syt1 by PKC affects synaptic transmission, we rescued *Syt1* knockout (KO) autaptic neurons with Semliki forest viral particles encoding wild-type Syt1 (Syt^{WT}) or nonphosphorylatable Syt1 (Syt^{T112A}, Fig. 1*B*). Syt^{T112A} had no effect on synaptic Syt1 levels, synapse number, or basal synaptic transmission (Fig. S1). Phorbol esters (synthetic DAG analogs) are widely used to activate the DAG/PKC pathway (3–5), and require the activation of PKC to potentiate vesicle release in hippocampal neurons (8). We therefore measured the effect of phorbol 12-myristate 13-acetate (PMA) in Syt^{WT} or Syt^{T112A} expressing neurons on spontaneous and AP-evoked release. PMA potently increased AP-evoked release (normalized amplitude in PMA = 1.53 ± 0.3, $P < 0.05$, Wilcoxon signed-rank test, $n = 13$, $n = 3$) and spontaneous release (normalized frequency in PMA = 1.7 ± 0.3, $P < 0.05$, $n = 12$, $n = 3$) in Syt^{WT}-expressing cells (Fig. 1 *C–F*), in line with previous studies (8, 10, 11). In contrast, PMA had no effect on excitatory postsynaptic current (EPSC) amplitude in Syt^{T112A}-expressing cells (normalized amplitude in PMA = 0.88 ± 0.3, $n = 14$, $P > 0.6$, Fig. 1 *C* and *D*), indicating that, like Munc18-1, phosphorylation of Syt1 is essential in this form of plasticity. Strikingly, potentiation of spontaneous release was still observed in neurons expressing Syt^{T112A}. Although potentiation was slightly delayed compared with Syt^{WT}, PMA application increased spontaneous release in Syt^{T112A}-expressing cells to frequencies comparable to Syt^{WT} (normalized frequency in PMA = 1.44 ± 0.3, $P < 0.05$ $n = 11$, Fig. 1 *E* and *F*). This suggests that phosphorylation of Syt1 is dispensable for PKC-dependent potentiation of spontaneous release.

It was previously shown that a phosphomimetic variant of Munc18 on its own does not potentiate evoked release, but supports PMA-induced potentiation (8). We therefore mutated T112 to aspartic acid (Syt^{T112D}, which presumably mimics the phosphorylated state) and tested its effect on PMA-induced potentiation. Syt^{T112D} fully supported potentiation of both spontaneous and evoked release (Fig. S2). These results demonstrate that phosphorylation of both Syt1 and Munc18-1 is required for potentiation of evoked release, whereas the phosphorylation of a single substrate is not sufficient for potentiation.

Previous studies showed that multiple Ca^{2+} sensors control spontaneous release, including Syt1 (15) and Doc2s (16, 17). We therefore hypothesized that in the absence of Syt1 phosphorylation, Doc2s mediate the increased spontaneous release. To test this, we repeated the PMA experiments in neurons obtained from *Doc2a/Doc2b/Syt1* triple knockout (TKO) mice (Fig. 1 *G–J*). As expected, Syt^{T112A} did not show potentiation of evoked release upon addition of PMA (Syt^{WT} 1.3 ± 1.0, $P < 0.05$ $n = 23$; Syt^{T112A} 1.0 ± 0.1, $n = 21$; $P > 0.9$ $n = 4$, Fig. 1 *G* and *H*). Importantly, the potentiation of spontaneous release was greatly reduced in TKO cells rescued with Syt^{T112A}, although some remaining potentiation was observed (Syt^{WT} 2.5 ± 0.5, $n = 14$; $P < 0.001$, Syt^{T112A} 1.5 ± 0.2, $P < 0.05$ $n = 13$, Fig. 1 *I* and *J*). Thus, phosphorylation of Syt1 at T112 potentiates both spontaneous and evoked release, but the effect on spontaneous release can be (partly) substituted by Doc2s and a fourth unidentified Ca^{2+} sensor.

Synaptotagmin-2 (Syt2) is a close homolog of Syt1 and acts as a Ca^{2+} sensor for synchronous release at multiple central synapses (23). Although Syt1 and Syt2 share high sequence homology, Syt2 strikingly lacks seven amino acid residues within the linker between TM and C2A, where the PKC/CaMK-II phosphorylation site in Syt1 resides (Fig. 1*K*). Previous studies demonstrated that Syt2-dependent synapses show normal phorbol-ester–induced potentiation (e.g., ref. 3). To test the effect of this deletion, we rescued *Syt1* KO cells with Syt2 or Syt1 with identical deletion ($Syt1^{\Delta 109–116}$, Fig. 1 *K–N*). Syt2 and $Syt1^{\Delta 109–116}$ rescued the AP-evoked EPSC to amplitudes comparable to $Syt1^{WT}$ (Fig. 1*M*). Moreover, both groups showed rapid and prominent facilitation of the EPSC upon addition of 1 µM phorbol 12,13-dibutyrate (PDBu) that exceeded potentiation in $Syt1^{WT}$ ($Syt1^{WT}$ 1.8 ± 0.2, $n = 13$ $P < 0.001$, $Syt2^{WT}$ 2.9 ± 0.4, $n = 12$ $Syt1^{\Delta 109–116}$ $P < 0.001$, 2.1 ± 0.3, $n = 14$ $P < 0.001$; Fig. 1*N*). This result suggests that this seven amino acid sequence within the linker of Syt1 has an inhibitory role at rest and becomes permissive of phorbol-ester–induced potentiation upon phosphorylation of T112.

Phosphorylation of Syt1 Enhances Potentiation After High-Frequency Stimulation. High-frequency stimulation (HFS) transiently potentiates the EPSC amplitude, which requires activation of PKC (6, 7, 11). We therefore hypothesized that phosphorylation of Syt1 might be important for this form of STP. First, we tested to what extent this form of STP can be induced in WT autaptic cultures. Using an induction protocol of 200 AP at 100 Hz, we found that 43% (3 of 7) of the cells displayed potentiation, whereas the remaining cells underwent transient depression (Fig. S3). This heterogeneity is not unexpected, because our cultures contain different types of glutamatergic neurons, including cells from CA1–3 and dentate gyrus. We then tested the effect of Syt1 phosphorylation using KO cells rescued with Syt^{WT} or Syt^{T112A}. For Syt^{WT}, we observed potentiation that was comparable to WT cells (Fig. 2 *A–C*). A total of 42% (13 of 30) of Syt^{WT} rescued cells displayed a transient increase in EPSC size, with potentiation

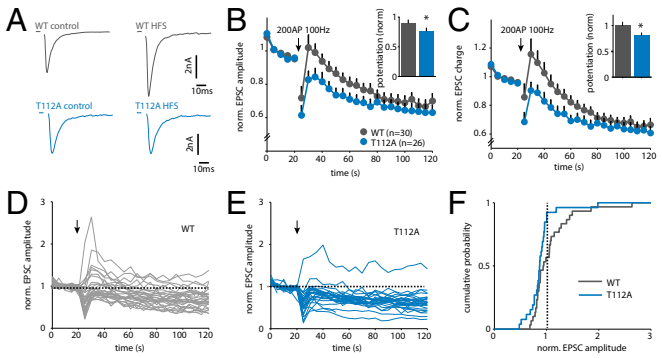

Fig. 2. Syt^{T112A} reduces potentiation after HFS. (*A*) Example traces of AP-evoked release in control and after stimulation with 200 AP at 100 Hz. (*B*) Effect of HFS on average normalized EPSC amplitude of all cells. *Inset* represents average change in EPSC amplitude of first 10 stimuli after 100-Hz train. (*C*) As in *B*, for average EPSC charge. (*D*) Normalized EPSC amplitudes of individual Syt^{WT} cells. Arrow indicates HFS. (*E*) Normalized EPSC amplitudes of individual Syt^{T112A} cells. Arrow indicates HFS. (*F*) Cumulative histogram of maximum change in normalized EPSC amplitude induced by HFS. Dotted line indicates amplitude = 1 (no change). $n = 2$. $^*P < 0.05$, Kruskal–Wallis ANOVA.

ranging from 6% to 170% (Fig. 2 *D* and *F*). In Syt^{T112A} rescued cells, however, potentiation was induced in only 7.7% (2 of 26) of the cells (Fig. 2 *A*–*C*, *E*, and *F*). Thus, although Syt1 phosphorylation is not strictly required, it strongly enhances potentiation after HFS.

Syt^{T112A} Does Not Prevent Potentiation of Vesicle Release Willingness. Phorbol esters are well known to potentiate release of primed vesicles induced by hypertonic sucrose. This potentiation relies on the activation of both Munc13 and PKC (8, 9, 24). We tested if Syt^{T112A} affects potentiation of the sucrose pool, by applying extracellular solution containing 250 mM sucrose (at which the PMA effect on sucrose-induced release is most pronounced; ref. 9). PMA significantly increased the sucrose response in Syt^{WT} cells from 3.8 ± 0.6–5.2 ± 1.0 nC (Fig. 3 *A*–*C*, $n = 2$). A similar effect was observed in cells expressing Syt^{T112A} (control, 4.0 ± 0.8 nC; PMA, 4.9 ± 1.0 nC).

The kinetics of sucrose-induced release are considered to be a measure for the release willingness of primed vesicles. Changes in release kinetics are observed upon DAG/PKC stimulation and interpreted as changes in the energy barrier for fusion during presynaptic plasticity (9, 25). Mutations in both Munc13-1 and Munc18-1 that prevent DAG/PKC-dependent activation change these kinetics (8, 9, 24). However, in contrast to Munc13-1 and Munc18-1 mutations, the kinetics of sucrose-induced release were similar for Syt^{WT} and Syt^{T112A} rescued neurons (Fig. 3*D*). As we observed above (Fig. 1), Syt^{T112A} did prevent potentiation of AP-evoked release in these cells (Fig. 3*E*). Thus, although Syt^{T112A} blocks potentiation of AP-evoked release, it does not do so by preventing the increase in release willingness known to occur during presynaptic plasticity.

Expression of a Nonphosphorylatable Mutant Does Not Prevent Phosphorylation of Other Substrates. We next tested if the introduction of a nonphosphorylatable mutant affects the phosphorylation of other PKC substrates. In theory, expression of a nonphosphorylatable mutant could create a "sink" for PKC, as PKC might remain bound to the mutated substrate. This situation might occur in experiments testing the two essential PKC substrates, Munc18-1 and Syt1. We therefore cultured *munc18-1* knockout neurons rescued with $Munc18\text{-}1^{WT}$ or nonphosphorylatable $Munc18\text{-}1^{3A}$ (8) in the presence of ^{32}P, and measured incorporation of ^{32}P into Syt1 after stimulation with PDBu (Fig. S4). *Munc18-1* neurons were used for this experiment because these neurons die in culture when not infected with virus encoding for Munc18 (8, 26). Thus, this ensures that 100% of the neurons express the given mutant, as opposed to ~80% rescue we typically reach in *syt1* knockout cultures. Surprisingly, we found that $Munc18\text{-}1^{3A}$ increases incorporation of ^{32}P, suggesting an increase in Syt1 phosphorylation. Thus, nonphosphorylatable mutants do not reduce phosphorylation of other available substrates and might even promote the local availability of PKC to phosphorylate other substrates.

Syt^{T112A} Does Not Affect Paired-Pulse Plasticity and Readily Releasable Vesicle Pool Size. The experiments in Fig. 1 suggest that, like Munc18-1, Syt1 is an essential substrate for PKC to potentiate synaptic transmission. We previously found that phosphorylation of Munc18-1 is critical for multiple forms of PKC-dependent plasticity, including paired-pulse plasticity and augmentation (8). To test if Syt^{T112A} also affects these forms of STP, we applied paired-pulse and train stimulation protocols to Syt^{WT} and Syt^{112A} rescued KO cells. No significant differences were observed in paired-pulse ratio at all intervals tested (20–1,000 ms), indicating that Syt^{T112A} has no effect on paired-pulse facilitation (Fig. 3 *F* and *G*). In addition, we did not observe an effect on the EPSC rundown during prolonged stimulation (100 AP at 40 Hz), or augmentation after this AP train (Fig. 3 *H* and *I*).

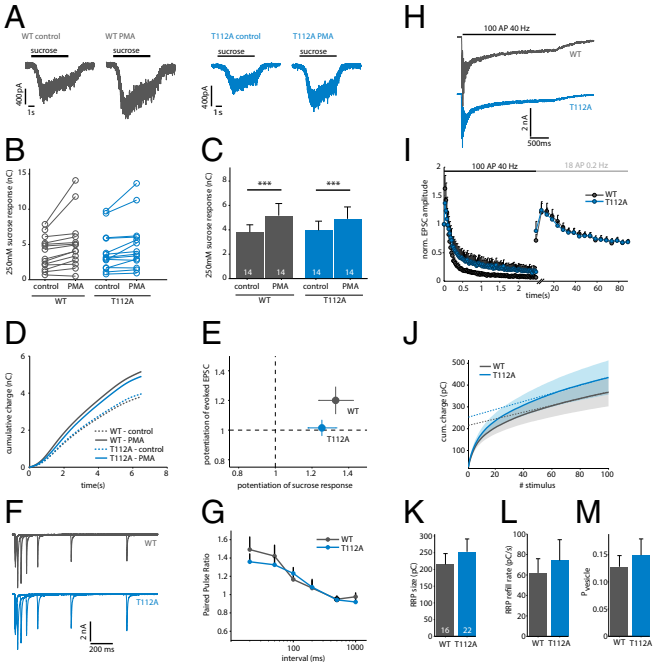

Fig. 3. Syt^{T112A} does not prevent potentiation of sucrose-induced release or STP. (*A*) Typical examples of responses to 250 mM sucrose in control and after superfusion with PMA. Black bars indicate sucrose application. (*B*) Effect of PMA on sucrose-induced release in individual cells. (*C*) Averages of the results in *B*. $^{***}P < 0.001$, Wilcoxon signed-rank test. (*D*) Average cumulative charge of the sucrose response in control and after superfusion with PMA. (*E*) Relationship between potentiation in AP-evoked and sucrose-evoked release by PMA in the same set of cells ($n = 2$). (*F*) Typical examples of a paired-pulse protocol with 20-, 50-, 100-, 200-, 500-, and 1,000-ms intervals. (*G*) Average paired-pulse ratio for each interval. Ratio was calculated as EPSC2/EPSC1 ($n = 3$). (*H*) Typical examples of EPSCs evoked by 100 AP at 40 Hz. Black bar indicates the AP train. (*I*) Normalized EPSC amplitude during 100 AP at 40 Hz and subsequent stimulation at 0.2 Hz. Black error bars represent SEM. (*J*) Cumulative charge of the synchronous EPSC during 100 AP at 40 Hz. Shaded area represents SEM; dotted lines denote a linear fit back extrapolated from the last 40 stimuli. (*K*) Average RRP size per cell, estimated by back extrapolation of the cumulative synchronous charge in *J* ($n = 3$). (*L*) RRP refilling rate during 40-Hz stimulation, estimated by the slope of back extrapolation. (*M*) Average vesicular release probability per cell, calculated as charge of first evoked divided by the RRP size.

NEUROSCIENCE

Thus, in contrast to Munc18-1, phosphorylation of Syt1 by PKC is not required for paired-pulse plasticity or Ca^{2+}-dependent refilling.

Furthermore, we tested if phosphorylation of Syt1 affects the size and refilling of the readily releasable vesicle pool (RRP). Back extrapolation of the cumulative charge measured during train stimulation is commonly used to estimate RRP size and refilling (27). With this method, we did not find significant differences in RRP size (Syt^{WT} 215.30 ± 32.3 pC, $n = 16$; Syt^{T112A} 252.9 ± 38.4 pC, $n = 22$, $n = 4$; Fig. 3 *J* and *K*). This is in line with previous studies reporting that DAG/PKC activation does not affect RRP size (3, 8, 9). The RRP refilling rate (Syt^{WT} 62.0 ± 13.9 pC/s; Syt^{T112A} 74.2 ± 20.3 pC/s; Fig. 3*L*), initial vesicular release probability (Syt^{WT} 0.13 ± 0.02; Syt^{T112A} 0.15 ± 0.03; Fig. 3*M*) and asynchronous release during the 40-Hz train (Syt^{WT} 2.5 ± 0.5 nC; Syt^{T112A} 3.0 ± 0.6 nC) were also similar. These results demonstrate that Syt^{T112A} does not affect RRP size and replenishment during and after stimulation at intermediate stimulation frequency.

Discussion

Activation of the DAG/PKC pathway acutely potentiates synaptic transmission, but the underlying mechanism is not completely understood. We discovered that phosphorylation of Syt1 is required for this pathway, as Syt^{T112A} abolished potentiation of evoked release by phorbol esters (Fig. 1) and severely reduced potentiation after HFS (Fig. 2). Because this mutation does not affect vesicle priming (Fig. 3), we propose that Syt1 phosphorylation controls a step downstream of priming to potentiate synaptic transmission.

Contribution of PKC to Potentiation of Release Is Cell-Type Specific. A previous study demonstrated that Syt^{T112A} does not affect vesicle release in chromaffin cells (21). Our results underscore that, despite many similarities, key differences exist between the release machineries of chromaffin cells and synapses (see also refs. 28 and 29). Although PMA potentiates release from embryonic chromaffin cells (21, 30), potentiation persists after inhibition of PKC (22), deletion of Munc18-1 (30), or rescue of Syt1-KO with Syt^{T112A} (21). In addition, the relative contribution of PKC to DAG-induced potentiation differs among synapses, as PKC activation is strictly required in hippocampal (6, 8), but not in Calyceal synapses (7, 11). This variation in PKC dependency is in line with the observation that a small population of cells did express potentiation after HFS in the absence of Syt1 phosphorylation (Fig. 2). The divergent effect of Syt^{T112A} in chromaffin cells and neurons is therefore most likely caused by unidentified differences in the release machineries of these cells.

Potentiation of Spontaneous Release Is Mediated by Multiple Ca^{2+} Sensors. Syt^{T112A} only reduced PMA-induced potentiation of spontaneous release when Doc2a and Doc2b were absent (Fig. 1). Syt1 and Doc2s all drive spontaneous release and compete for SNARE complex binding (15–17). Our data indicate that potentiation of spontaneous release is independently supported by multiple Ca^{2+} sensors, underscoring the molecular redundancy in spontaneous vesicle fusion (reviewed in ref. 31). Doc2s are not known PKC substrates, and thus the increased spontaneous release is likely caused by the activation of Munc13-1 and Munc18-1, or a yet unidentified PKC substrate, and is independent of Syt1 phosphorylation (Fig. 4). A plausible scenario is that Munc13-1/Munc18-1 activation leads to a situation where vesicles are more likely to fuse than under resting conditions (higher "fusogenicity" or "fusion willingness") and alternate sensors, phosphorylated Syt1 or Doc2s, are more likely to trigger fusion upon spontaneous fluctuations in presynaptic Ca^{2+} (in the absence of action potentials).

Syt1 Phosphorylation Is Dispensable During Paired-Pulse Plasticity. During paired-pulse plasticity, neurons expressing Syt^{T112A} were indistinguishable from Syt^{WT} (Fig. 3). Interestingly, mutations in the other two elements of the secretion machinery known to be essential in the DAG/PKC pathway, Munc13-1 or Munc18-1, did inhibit paired-pulse plasticity (8, 10). Partial summation of intracellular Ca^{2+} transients during paired stimuli ("residual Ca^{2+}") was recently shown to activate synaptotagmin-7 in addition to Syt1 and to be responsible for paired-pulse plasticity (32). Competition between sensors and/or residual Ca^{2+} itself may render Syt1 phosphorylation redundant during paired stimuli, whereas Munc13-1 and Munc18-1 activation remains essential. Potentiation after HFS, on the other hand, decays much slower than residual Ca^{2+} (33, 34) and appears to be at least a partially distinct process (discussed in ref. 2). Under these conditions, syt1 phosphorylation is required to produce full potentiation (Fig. 2).

Distinct Actions of Syt1 and Other Known Factors in the DAG/PKC Pathway. It is incompletely understood how the currently known critical factors for STP, Munc13, PKC, and Munc18-1, establish

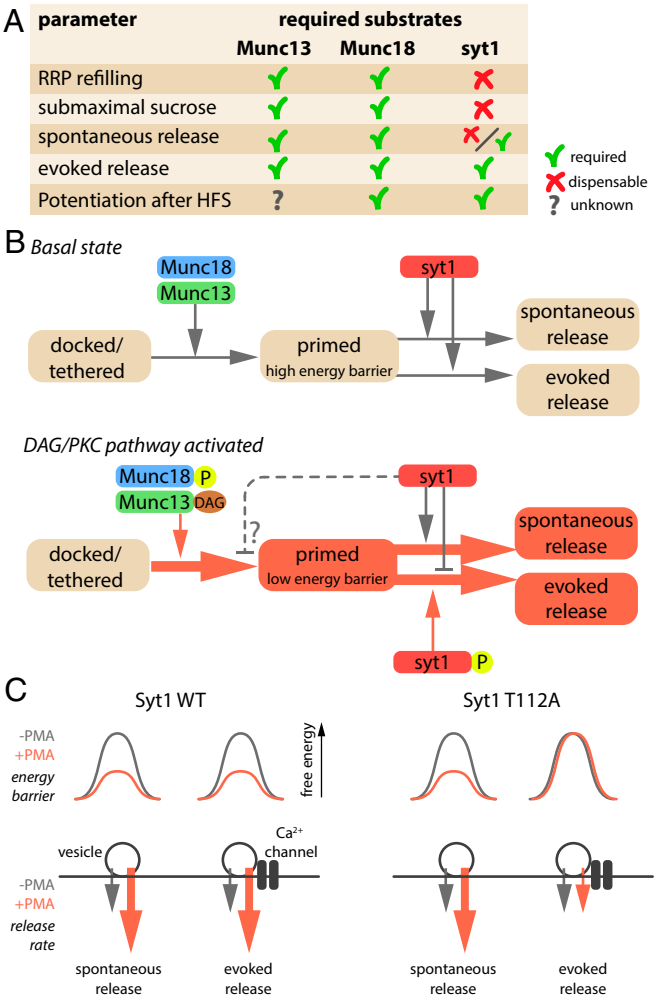

Fig. 4. Working model for DAG/PKC-induced potentiation of vesicle fusion. (*A*) Overview of synaptic parameters potentiated by the DAG/PKC pathway and the required substrates for each parameter. Syt1 data are derived from the current study; Munc18-1 data from refs. 8 and 12; and Munc13 data from refs. 9–11. (*B*) Proposed working model for DAG/PKC-induced potentiation. Activation of Munc13-1 and Munc18-1 potentiates vesicle priming while lowering the fusion barrier, making vesicles more fusogenic (red color box) compared with the basal state. Syt1 appears to inhibit the AP-induced evoked release, but not spontaneous release, of these highly fusogenic vesicles or may even prevent the increase in fusogenicity of specific vesicles used in AP-induced release (dashed line). (*C*) Working model to explain the fact that AP-induced release is not potentiated by DAG in synapses expressing Syt^{T112A}, whereas the overall fusogenicity of vesicles is increased by DAG. A subset of vesicles, preferentially used by AP-induced release may be exempt from potentiation and have a normal energy barrier, despite the fact that DAG has lowered the barrier for most vesicles. In this hypothetical model, Syt1 would also influence priming (dashed line in *B*).

different types of STP and it is therefore difficult to assess how the role of Syt1 phosphorylation feeds into this. Most studies agree that the RRP size remains unaltered during STP in synapses studied so far (discussed in ref. 9). Hence, the DAG/PKC pathway may not change the number of release sites and STP should be explained by molecular changes that facilitate release site refilling and/or downstream changes, such as increased priming rates and/or fusion probability.

Because PKC phosphorylation of Munc18-1 and Syt1, and activation of Munc13-1, are all essential for DAG-induced potentiation, the simplest scenario would be that these three factors act interdependently at the same step. However, mutations in these molecules that prevent DAG-induced potentiation do not produce exact phenocopies in all STP experiments (Fig. 4*A*). Paired-pulse plasticity critically depends on activation of Munc13-1 and PKC and PKC phosphorylation of Munc18-1, but Syt1 phosphorylation is dispensable (see above); potentiation by direct application of DAG (-analogs) depends on all these factors (8, 11, 12) and HFS-induced potentiation requires at least PKC activation (6, 7, 35), Munc18-1 phosphorylation (12), and Syt1 phosphorylation (Fig. 2), whereas the role of Munc13-1 is unknown. Finally, further differences were exposed in assays to probe the underlying biophysical principles of STP: accelerated RRP refilling after 40-Hz stimulation and accelerated synaptic responses to hypertonic sucrose are known features of DAG/PKC and depend on activation of Munc13-1 and PKC and PKC phosphorylation of Munc18-1 (8–10), but Syt1 phosphorylation is dispensable (Fig. 3).

It has been suggested that Syt1 phosphorylation increases binding to SNARE proteins (36). However, recent studies using high-resolution NMR (37) and crystallography (38) suggest that the C2 domains of Syt1 mediate SNARE binding, making it unlikely that PKC-dependent changes in the linker affect SNARE binding directly. However, it was recently suggested that the linker undergoes a structural change (39) and might become sterically able to engage the SNAREs or membranes without any change in the bimolecular affinity as such. The linker region may also affect Syt1's oligomerization (40). PKC-mediated phosphorylation may modulate these properties and hereby regulate potentiation.

Previous studies have provided some insight in the molecular role of other essential DAG/PKC effectors. DAG binding to Munc13-1 is thought to disinhibit its catalytic MUN domain (9), which facilitates the transition from the syntaxin–Munc18-1 dimer to a (partially) assembled SNARE complex (41). PKC-dependent phosphorylation of Munc18-1 might further accelerate this transition, by decreasing syntaxin–Munc18-1 binding (42, 43). In this way, Munc13-1 activation and Munc18-1 phosphorylation may together facilitate RRP refilling after intense stimulation. This scenario may explain why Munc13-1 or Munc18-1 mutations that block the DAG pathway do not show enhanced RRP refilling after 40-Hz stimulation (8, 10). However, this aspect of STP is unaffected in neurons expressing Syt^{T112A}, implying that Munc13-1 and Munc18-1 still facilitate RPP refilling when Syt1 phosphorylation is blocked. This suggests that Syt1 phosphorylation acts downstream of Munc13-1 and Munc18-1 (Fig. 4*B*).

This conclusion is also supported by differences in synaptic responses to hypertonic sucrose. Synapses expressing Munc13-1 or Munc18-1 mutations that block the DAG-induced potentiation prevent the characteristic DAG-dependent acceleration of sucrose responses (8, 9), but Syt^{T112A} expressing synapses show normal acceleration (Fig. 3). Synaptic responses to hypertonic sucrose are a poorly understood, but well-validated phenomenon used to probe the fusogenicity of synaptic vesicles, i.e., the energy barrier for fusion (9, 25, 44). Potentially, DAG-dependent enhancement of Munc13-1 and Munc18-1's role in setting up SNARE complexes results in a higher number of SNARE complexes per vesicle, leading to a higher fusogenicity. In such a scenario, the Syt^{T112A} mutation will not affect DAG-dependent acceleration of synaptic responses to hypertonic sucrose because it is a Ca^{2+}-independent stimulus, bypassing natural Ca^{2+}-dependent fusion triggering. Alternatively, DAG-dependent conformational changes in Munc13-1 or Munc18-1 may also directly increase fusogenicity (i.e., without changing SNARE stoichiometry).

Syt^{T112A} does not prevent the DAG-dependent increase in fusogenicity (accelerated RRP refilling and responses to sucrose), but does prevent DAG-dependent potentiation of AP-evoked release. This implies that Syt1 has an intrinsic inhibitory effect on DAG-dependent potentiation of evoked release, reversed by T112 phosphorylation (Fig. 4*B*). This conclusion is further substantiated by the fact that deletion of the linker region in Syt1 ($Syt1^{\Delta 109–116}$) or expression of Syt2 in Syt1 KO synapses supported normal DAG-induced potentiation. Both $Syt1^{\Delta 109–116}$ and Syt2 lack the sequence flanking T112, and this would relieve the inhibitory role of Syt1 in plasticity. Hence, Syt^{T112A} prevents potentiation of AP-induced release, despite the fact that vesicles generally have a higher fusogenicity. This inhibitory effect does not affect basal synaptic transmission, only DAG-dependent potentiation. This suggests that vesicles are in different states before and during DAG-dependent potentiation, because only in the latter case their release can be inhibited by preventing Syt1 phosphorylation (Fig. 4*B*). One explanation for these observations would be that vesicles preferentially fusing during AP-induced release (closest to Ca^{2+} channels) are biochemically different from most other vesicles and do not have increased fusogenicity. This working model is depicted in Fig. 4*C*. In this hypothetical scenario, Syt1 phosphorylation does not only act downstream of Munc13-1 and Munc18-1, but also at the priming step (dashed line in Fig. 4*B*).

Together, we propose that the substrates of the DAG/PKC pathway potentiate synaptic transmission by acting on a single cellular pathway that enhances priming rates and increases fusogenicity. Munc13-1 and Munc18-1 activation enhance priming rates in an interdependent manner, maybe by setting up trans-SNARE complexes faster, and increase fusiogenicity by setting up more complexes per vesicle or by unknown direct actions on the fusion barrier. However, vesicles used by AP-induced release appear to be exempt from potentiation as long as Syt1 is not phosphorylated.

Methods

Cell Culture and Viral Transduction. Autaptic hippocampal neurons were cultured from embryonic day 18 (E18) pups from previously documented mouse lines [*Syt1* knockout (KO) or *Syt1*/*Doc2a*/*Doc2b* TKO mice (14, 16, 45) or C57BL/6] as described (46). Cultures were grown in Neurobasal supplemented with 2% B27, 1.8% Hepes, 0.5% GlutaMAX, and 0.1% penicillin/streptomycin (all obtained from Invitrogen). Animals were housed and bred according to institutional guidelines and Dutch law, and all experiments were approved by the institutional animal committee of VU University and VU Medical Center. Semliki forest viral particles encoding for Syt1 (wt)-IRES-eGFP, Syt1(T112A)-IRES-eGFP, or Syt1(T112D)-IRES-eGFP, Syt2(wt)-IRES-eGFP, or Syt1(Δ109–116)-IRES-eGFP (21) were produced as described (47). Viral transduction was performed 16 h before start of the experiment. Lentiviral particles encoding for Munc18(wt)GFP, Munc18(3A)GFP (8), Syt1(wt)-IRES-eGFP, Syt2(wt)-IRES-eGFP, or Syt1(Δ109–116)-IRES-eGFP were produced as described (48). Lentiviral transduction was performed on day in vitro (DIV)2–4.

Electrophysiology. Whole-cell recordings were performed at room temperature (20–23 °C) at 13–16 DIV with borosilicate glass pipettes (2–4 MΩ) containing 125 mM K^+-gluconic acid, 10 mM NaCl, 4.6 mM $MgCl_2$, 4 mM K_2-ATP, 1 mM creatine phosphate, 1 mM EGTA, and 20 units/mL phosphocreatine kinase, pH = 7.3 and extracellular solution containing 140 mM NaCl, 2.4 mM KCl, 4 mM $CaCl_2$, 4 mM $MgCl_2$, 10 mM Hepes and 10 mM glucose, pH = 7.3. Cells were kept in voltage clamp (V_m = −70 mV) using an Axopatch 200B amplifier (Axon Instruments). Series resistance was 90% compensated (20-μs lag). APs were induced by 0.5-ms steps to 30 mV. Signals were recorded with Digidata 1440A and pCLAMP 10 software (both Axon Instruments). A total of 1 μM PMA (Tocris) was perfused onto the sample for 2 min; PDBu (Sigma) was bath applied to a final concentration of 1 μM. No perfusion was used to wash out phorbol esters after application had ended. Hypertonic sucrose (250 mM, Applichem) was applied for 5.5 s using a piezo-controlled barrel application system (Perfusion Fast-Step, Warner Instruments). The integral of the entire EPSC was used as measure for the sucrose response. Although this overestimates the sucrose-pool size, it was preferred because under our conditions, submaximal sucrose concentrations do not result in a clear "peak" response (Fig. 3*A*) that is considered to represent the true sucrose pool (9). Acquired signals were analyzed in MiniAnalysis 6 (Synaptosoft) and custom written programs in Matlab (Mathworks). In all figures, stimulation artifacts have been blanked out.

Immunocytochemistry and Confocal Microscopy. Cultures were fixed at 14 DIV with 4% (vol/vol) formaldehyde and stained as described previously (49). Primary antibodies and dilution used: chicken anti-MAP (1:10,000; Abcam), guinea pig anti-vGlut1 (1:5,000; Millipore), and rabbit anti–synaptotagmin-1 (1:2,000; W855; a gift from T. C. Sudhof, Stanford University). Samples were examined on a confocal microscope (LSM510, Zeiss). Images were acquired with a 40× oil objective (N.A. 1.3) and 0.7× mechanical zoom. Neuronal morphology and synaptic protein levels were measured using the semiautomated Matlab routine SynD (50).

In Vivo Phosphorylation Assay and Western Blotting. Hippocampal neurons derived from E18 *munc18-1* knockout mice (51) were cultured on poly-ornithin/laminin coating (2,000 K per condition in 10-cm dishes) and rescued with lentiviruses encoding Munc18(wt) or Munc18(3A). On DIV 14–16, cells were labeled for 4 h with 0.5 mCi/mL orthophosphate (NEX053S010MC, Perkin Elmer) in DMEM without phosphate (Gibco). After stimulation with 1 μM okadeic acid, 1 μM PDBu or DMSO, cells were washed once with DMEM without phosphate and lysed in 1× Laemmli sample buffer [2% (wt/vol) SDS, 10% (vol/vol) glycerol, 0.26 M B-mercaptoethanol, 60 mM Tris·HCl, pH 6.8]. After boiling, samples were diluted 15 times in immunoprecipitation (IP) buffer (50 mM Tris·HCl, pH 7.5, 1% Triton X-100, 1.5 mM $MgCl_2$, 5.0 mM EDTA, 100 mM NaCl). For binding, antibodies against Munc18 (BD Transduction Laboratories) or Syt1 (BD Transduction Laboratories) and Magnetic ProteinA beads (Millipore) were added and the samples were tumbled 16 h at 4 °C. After five washes with IP buffer, samples were eluted from the beads with Laemmli sample buffer and analyzed with SDS/PAGE. Cells were exposed for 7 d and phosphoimages were made with Image Reader FLA-5000 (Fuji). Immunoblots were stained for Munc18 and Syt1. Secondary antibodies were conjugated with alkaline phosphatase and Attophos (Promega) was used as substrate. Blots were imaged with Image Reader FLA-5000 (Fuji).

Statistics. Statistical significance between experimental groups was determined with a Kruskal–Wallis test. The effect of PMA was tested using a Wilcoxon signed rank test. All tests were performed in Matlab, assuming significance if $P < 0.05$. All data are represented as averages; error bars represent the SEM. *N* indicates the number of separate preparations and *n*, the number of observations.

ACKNOWLEDGMENTS. We thank Robbert Zalm for expert help with virus production, cloning, and performing some of the radioactive experiments; Desiree Schut for preparing glia feeders and culturing neurons; and Joost Hoetjes, Joke Wortel, Christiaan van der Meer, and Frank den Oudsten for breeding and genotyping mutant mice. This work is supported by the Netherlands Organization for Scientific Research ZonMw-VENI 916-66-101 and ZonMW-TOP 91208017 (to R.F.G.T.) and Pionier/VICI 900-01-001 and ZonMW 903-42-095 (to M.V.) and by the European Union ERC Advanced Grant 322966, HEALTH-F2-2009-241498 EUROSPIN, and HEALTH-F2-2009-242167 SynSys (to M.V.).

1. de Jong AP, Verhage M (2009) Presynaptic signal transduction pathways that modulate synaptic transmission. *Curr Opin Neurobiol* 19(3):245–253.
2. Zucker RS, Regehr WG (2002) Short-term synaptic plasticity. *Annu Rev Physiol* 64:355–405.
3. Lou X, Scheuss V, Schneggenburger R (2005) Allosteric modulation of the presynaptic Ca2+ sensor for vesicle fusion. *Nature* 435(7041):497–501.
4. Malenka RC, Madison DV, Nicoll RA (1986) Potentiation of synaptic transmission in the hippocampus by phorbol esters. *Nature* 321(6066):175–177.
5. Shapira R, Silberberg SD, Ginsburg S, Rahamimoff R (1987) Activation of protein kinase C augments evoked transmitter release. *Nature* 325(6099):58–60.
6. Brager DH, Cai X, Thompson SM (2003) Activity-dependent activation of presynaptic protein kinase C mediates post-tetanic potentiation. *Nat Neurosci* 6(6):551–552.
7. Fioravante D, Chu Y, Myoga MH, Leitges M, Regehr WG (2011) Calcium-dependent isoforms of protein kinase C mediate posttetanic potentiation at the calyx of Held. *Neuron* 70(5):1005–1019.
8. Wierda KD, Toonen RF, de Wit H, Brussaard AB, Verhage M (2007) Interdependence of PKC-dependent and PKC-independent pathways for presynaptic plasticity. *Neuron* 54(2): 275–290.
9. Basu J, Betz A, Brose N, Rosenmund C (2007) Munc13-1 C1 domain activation lowers the energy barrier for synaptic vesicle fusion. *J Neurosci* 27(5):1200–1210.
10. Rhee JS, et al. (2002) Beta phorbol ester- and diacylglycerol-induced augmentation of transmitter release is mediated by Munc13s and not by PKCs. *Cell* 108(1):121–133.
11. Lou X, Korogod N, Brose N, Schneggenburger R (2008) Phorbol esters modulate spontaneous and Ca2+-evoked transmitter release via acting on both Munc13 and protein kinase C. *J Neurosci* 28(33):8257–8267.
12. Genc O, Kochubey O, Toonen RF, Verhage M, Schneggenburger R (2014) Munc18-1 is a dynamically regulated PKC target during short-term enhancement of transmitter release. *eLife* 3:e01715.
13. Hilfiker S, Pieribone VA, Nordstedt C, Greengard P, Czernik AJ (1999) Regulation of synaptotagmin I phosphorylation by multiple protein kinases. *J Neurochem* 73(3):921–932.
14. Geppert M, et al. (1994) Synaptotagmin I: A major Ca2+ sensor for transmitter release at a central synapse. *Cell* 79(4):717–727.
15. Xu J, Pang ZP, Shin OH, Südhof TC (2009) Synaptotagmin-1 functions as a Ca2+ sensor for spontaneous release. *Nat Neurosci* 12(6):759–766.
16. Groffen AJ, et al. (2010) Doc2b is a high-affinity Ca2+ sensor for spontaneous neurotransmitter release. *Science* 327(5973):1614–1618.
17. Pang ZP, et al. (2011) Doc2 supports spontaneous synaptic transmission by a Ca(2+)-independent mechanism. *Neuron* 70(2):244–251.
18. Popoli M (1993) Synaptotagmin is endogenously phosphorylated by Ca2+/calmodulin protein kinase II in synaptic vesicles. *FEBS Lett* 317(1–2):85–88.
19. Kaeser-Woo YJ, et al. (2013) Synaptotagmin-12 phosphorylation by cAMP-dependent protein kinase is essential for hippocampal mossy fiber LTP. *J Neurosci* 33(23):9769–9780.
20. Wu B, et al. (2015) Synaptotagmin-7 phosphorylation mediates GLP-1-dependent potentiation of insulin secretion from β-cells. *Proc Natl Acad Sci USA* 112(32):9996–10001.
21. Nagy G, et al. (2006) Different effects on fast exocytosis induced by synaptotagmin 1 and 2 isoforms and abundance but not by phosphorylation. *J Neurosci* 26(2):632–643.
22. Nili U, et al. (2006) Munc18-1 phosphorylation by protein kinase C potentiates vesicle pool replenishment in bovine chromaffin cells. *Neuroscience* 143(2):487–500.
23. Pang ZP, Südhof TC (2010) Cell biology of Ca2+-triggered exocytosis. *Curr Opin Cell Biol* 22(4):496–505.
24. Stevens CF, Sullivan JM (1998) Regulation of the readily releasable vesicle pool by protein kinase C. *Neuron* 21(4):885–893.
25. Schotten S, et al. (2015) Additive effects on the energy barrier for synaptic vesicle fusion cause supralinear effects on the vesicle fusion rate. *eLife* 4:e05531.
26. Heeroma JH, et al. (2004) Trophic support delays but does not prevent cell-intrinsic degeneration of neurons deficient for munc18-1. *Eur J Neurosci* 20(3):623–634.
27. Schneggenburger R, Meyer AC, Neher E (1999) Released fraction and total size of a pool of immediately available transmitter quanta at a calyx synapse. *Neuron* 23(2):399–409.
28. de Wit H, Cornelisse LN, Toonen RF, Verhage M (2006) Docking of secretory vesicles is syntaxin dependent. *PLoS One* 1:e126.
29. Gerber SH, et al. (2008) Conformational switch of syntaxin-1 controls synaptic vesicle fusion. *Science* 321(5895):1507–1510.
30. Gulyás-Kovács A, et al. (2007) Munc18-1: Sequential interactions with the fusion machinery stimulate vesicle docking and priming. *J Neurosci* 27(32):8676–8686.
31. Walter AM, Groffen AJ, Sørensen JB, Verhage M (2011) Multiple Ca2+ sensors in secretion: Teammates, competitors or autocrats? *Trends Neurosci* 34(9):487–497.
32. Jackman SL, Turecek J, Belinsky JE, Regehr WG (2016) The calcium sensor synaptotagmin 7 is required for synaptic facilitation. *Nature* 529(7584):88–91.
33. Bai J, Wang CT, Richards DA, Jackson MB, Chapman ER (2004) Fusion pore dynamics are regulated by synaptotagmin*t-SNARE interactions. *Neuron* 41(6):929–942.
34. Regehr WG, Delaney KR, Tank DW (1994) The role of presynaptic calcium in short-term enhancement at the hippocampal mossy fiber synapse. *J Neurosci* 14(2):523–537.
35. Korogod N, Lou X, Schneggenburger R (2007) Posttetanic potentiation critically depends on an enhanced Ca(2+) sensitivity of vesicle fusion mediated by presynaptic PKC. *Proc Natl Acad Sci USA* 104(40):15923–15928.
36. Verona M, Zanotti S, Schäfer T, Racagni G, Popoli M (2000) Changes of synaptotagmin interaction with t-SNARE proteins in vitro after calcium/calmodulin-dependent phosphorylation. *J Neurochem* 74(1):209–221.
37. Brewer KD, et al. (2015) Dynamic binding mode of a Synaptotagmin-1-SNARE complex in solution. *Nat Struct Mol Biol* 22(7):555–564.
38. Zhou Q, et al. (2015) Architecture of the synaptotagmin-SNARE machinery for neuronal exocytosis. *Nature* 525(7567):62–67.
39. Lai Y, Lou X, Jho Y, Yoon TY, Shin YK (2013) The synaptotagmin 1 linker may function as an electrostatic zipper that opens for docking but closes for fusion pore opening. *Biochem J* 456(1):25–33.
40. Lu B, Kiessling V, Tamm LK, Cafiso DS (2014) The juxtamembrane linker of full-length synaptotagmin 1 controls oligomerization and calcium-dependent membrane binding. *J Biol Chem* 289(32):22161–22171.
41. Ma C, Li W, Xu Y, Rizo J (2011) Munc13 mediates the transition from the closed syntaxin-Munc18 complex to the SNARE complex. *Nat Struct Mol Biol* 18(5):542–549.
42. Barclay JW, et al. (2003) Phosphorylation of Munc18 by protein kinase C regulates the kinetics of exocytosis. *J Biol Chem* 278(12):10538–10545.
43. de Vries KJ, et al. (2000) Dynamics of munc18-1 phosphorylation/dephosphorylation in rat brain nerve terminals. *Eur J Neurosci* 12(1):385–390.
44. Rosenmund C, Stevens CF (1996) Definition of the readily releasable pool of vesicles at hippocampal synapses. *Neuron* 16(6):1197–1207.
45. Sakaguchi G, et al. (1999) Doc2alpha is an activity-dependent modulator of excitatory synaptic transmission. *Eur J Neurosci* 11(12):4262–4268.
46. Meijer M, et al. (2012) Munc18-1 mutations that strongly impair SNARE-complex binding support normal synaptic transmission. *EMBO J* 31(9):2156–2168.
47. Voets T, et al. (2001) Munc18-1 promotes large dense-core vesicle docking. *Neuron* 31(4):581–591.
48. Naldini L, et al. (1996) In vivo gene delivery and stable transduction of nondividing cells by a lentiviral vector. *Science* 272(5259):263–267.
49. de Jong AP, Schmitz SK, Toonen RF, Verhage M (2012) Dendritic position is a major determinant of presynaptic strength. *J Cell Biol* 197(2):327–337.
50. Schmitz SK, et al. (2011) Automated analysis of neuronal morphology, synapse number and synaptic recruitment. *J Neurosci Methods* 195(2):185–193.
51. Verhage M, et al. (2000) Synaptic assembly of the brain in the absence of neurotransmitter secretion. *Science* 287(5454):864–869.